The Astrophysical Journal, 687:532–541, 2008 November 1

FAR ULTRAVIOLET SPECTROSCOPIC EXPLORER SPECTROSCOPY OF THE NOVA-LIKE CATACLYSMIC VARIABLE BB DORADUS[1]

Patrick Godon[2] and Edward M. Sion
Department of Astronomy and Astrophysics, Villanova University, Villanova, PA 19085; patrick.godon@villanova.edu, edward.sion@villanova.edu

Paul E. Barrett
United States Naval Observatory, Washington, DC 20392; barrett.paul@usno.navy.mil

Paula Szkody
Department of Astronomy, University of Washington, Seattle, WA 98195; szkody@astro.washington.edu

and

Eric M. Schlegel
Department of Physics and Astronomy, University of Texas, San Antonio, TX 78249; eric.schlegel@utsa.edu
Received 2008 May 2; accepted 2008 June 27

ABSTRACT

We present an analysis of the *Far Ultraviolet Spectroscopic Explorer* (*FUSE*) spectra of the little-known southern nova-like cataclysmic variable, BB Doradus. The spectrum was obtained as part of our Cycle 8 *FUSE* survey of high-declination nova-like stars. The *FUSE* spectrum of BB Dor, observed in a high state, is modeled with an accretion disk with a very low inclination (possibly lower than 10°). Assuming an average white dwarf (WD) mass of $0.8\,M_{\odot}$ leads to a mass accretion rate of $10^{-9}\,M_{\odot}\,\mathrm{yr}^{-1}$ and a distance on the order of $\sim$650 pc, consistent with the extremely low Galactic reddening in the direction of BB Dor. The spectrum presents some broad and deep silicon and sulfur absorption lines, indicating that these elements are overabundant by 3 and 20 times solar, respectively.

Subject headings: accretion, accretion disks — novae, cataclysmic variables — stars: abundances — stars: individual (BB Doradus) — white dwarfs

Online material: color figures

1. INTRODUCTION

1.1. *Nova-like Cataclysmic Variables*

Cataclysmic variables (CVs) are close binaries in which the primary, a white dwarf (WD), accretes matter and angular momentum from the secondary, a main-sequence star, filling its Roche lobe. The matter is transferred by means of either an accretion disk around the WD or an accretion column, formed when the WD has a strong ($\sim$10 MG) magnetic field. Ongoing accretion at a low rate (quiescence) is interrupted every few weeks to months by intense accretion (outburst) of days to weeks (a dwarf nova accretion event), and every few thousand years by a thermonuclear explosion (TNR; the classical nova event). CV systems are divided into subclasses according to the duration, occurrence, and amplitude of their outbursts: dwarf novae (DNs) are found mostly in the low state, while nova-like CVs (NLs) exhibit the spectroscopic and photometric characteristics of novae between or after outbursts, but have never had a recorded outburst. NLs form a less homogeneous class and are divided into subtypes depending on certain properties, such as eclipsing systems, magnetic systems, or systems that go into unexpected low states (Warner 1995). Nonmagnetic NLs can be divided into UX UMa systems, which remain in a state of high optical brightness or a "permanent outburst state," and VY Scl systems (anti–dwarf novae), which experience unexpected low states when the optical brightness plummets.

CVs are believed to evolve from long period ($\sim$2 days) toward short period ($\sim$1 hr) as the mass ratio q decreases, crossing the 2–3 hr "period gap," where few systems are found. Theory predicts that the period of those systems with a sufficiently low q will increase as q continues to decrease, producing the so-called "period bouncers" (Patterson et al. 2005a). The driving mechanism behind the mass transfer ($\dot{M}$) and hence, the evolution of CVs, is believed to be angular momentum loss, dominated by magnetic stellar wind braking at periods above 3 hr and by gravitational wave emission below this period. The secondaries are stripped to $<0.08\,M_{\odot}$ on a timescale of only 1–4 Gyr after they form as close binaries above the gap. Consequently, in the lifetime of the Galaxy, the vast majority of CVs should have evolved to a period minimum near 80 minutes, and should now have degenerate brown dwarflike secondaries (Howell et al. 2001). However, recent models (Andronov et al. 2003) suggest (1) much lower angular momentum loss rates, such that it takes 10–12 Gyr to even reach a 3 hr period, and (2) multiple evolutionary tracks yielding different populations of CVs above and below the 3 hr orbital period.

The accretion disks and underlying accreting WDs in CVs can provide crucial clues and constraints on these evolutionary scenarios. It is important to derive $\dot{M}$ from observations, as the mass transfer rate is tied to the angular momentum loss. As to the WDs, they are the central engines of the observed outbursts, either as potential wells for the release of accretional energy or as the sites of

[1] Based on observations made with the NASA-CNES-CSA *Far Ultraviolet Spectroscopic Explorer*, which is operated for NASA by the Johns Hopkins University under NASA contract NAS5-32985.

[2] Visiting at the Space Telescope Science Institute, Baltimore, MD 21218; godon@stsci.edu.

Report Documentation Page

Form Approved
OMB No. 0704-0188

1. REPORT DATE	2. REPORT TYPE	3. DATES COVERED
01 NOV 2008		**00-00-2008 to 00-00-2008**

4. TITLE AND SUBTITLE	5a. CONTRACT NUMBER
Far Ultraviolet Spectroscopic Explorer Spectroscopy of the Nova-Like Cataclysmic Variable BB Doradus	5b. GRANT NUMBER
	5c. PROGRAM ELEMENT NUMBER
6. AUTHOR(S)	5d. PROJECT NUMBER
	5e. TASK NUMBER
	5f. WORK UNIT NUMBER
7. PERFORMING ORGANIZATION NAME(S) AND ADDRESS(ES) **Department of Astronomy and Astrophysics,Villanova University,Villanova,PA,19085**	8. PERFORMING ORGANIZATION REPORT NUMBER
9. SPONSORING/MONITORING AGENCY NAME(S) AND ADDRESS(ES)	10. SPONSOR/MONITOR'S ACRONYM(S)
	11. SPONSOR/MONITOR'S REPORT NUMBER(S)

12. DISTRIBUTION/AVAILABILITY STATEMENT
Approved for public release; distribution unlimited

13. SUPPLEMENTARY NOTES

14. ABSTRACT

15. SUBJECT TERMS

16. SECURITY CLASSIFICATION OF:			17. LIMITATION OF ABSTRACT	18. NUMBER OF PAGES	19a. NAME OF RESPONSIBLE PERSON
a. REPORT **unclassified**	b. ABSTRACT **unclassified**	c. THIS PAGE **unclassified**	**Same as Report (SAR)**	**10**	

explosive TNR shell burning. In addition, the differences between the temperatures, rotation, and chemical abundances of CV WDs and single isolated WDs provide clues as to the effects of accretion, diffusion, and long-term heating and evolution (Sion 1995).

With a wavelength range of 905–1187 Å, the *Far Ultraviolet Spectroscopic Explorer* (*FUSE*) covers that part of the far-ultraviolet (FUV) spectrum where the hotter CV component is dominant. For NLs, the dominant component in the *FUSE* range is usually the accretion disk. Additional possible components are the hot white dwarf, the boundary layer or accretion belt, and other hot regions on or close to the WD. Many CV FUV spectra are modeled with two components, usually a WD plus a disk. For each system, one usually derives from the *FUSE* spectrum the temperature of the WD ($T_{\rm eff}$), the gravity, the rotational velocity ($V_{\rm rot}$ sin i), the chemical abundances, the mass accretion rate, the inclination, and the distance to the system.

It has therefore been very important to try to obtain *FUSE* data for more CV systems, in order to populate the $T_{\rm eff}$-period and the $\dot{M}$-period parameter spaces. There is a need to enlarge the sample to obtain an accurate global picture of the systems above and below the period gap. For that reason, we proposed to observe with *FUSE* a set of 16 high-declination dwarf novae (our Cycle 7 survey of DNs) and 16 high-declination NLs (our Cycle 8 survey of NLs, all chosen from the online CV catalog of Downes et al.). Unfortunately, our *FUSE* NL survey was cut short due to the fatal failure of the reaction wheel of the telescope. Of the 16 targets, only two were observed: BB Dor and P831-57. The analysis of the *FUSE* spectrum of P831-57 is presented elsewhere (P. Barrett et al. 2008, in preparation). In this work, we present the result of the *FUSE* spectroscopic analysis of BB Dor.

1.2. *The Nova-like CV BB Doradus*

BB Dor (also known as EC 05287−5847, an object from the Edinburgh-Cape Survey [Chen et al. 2001]) was spectroscopically identified as a CV in 1987 December, and was seen fainter than $V \sim 16.5$ until 1992 November (Chen et al. 2001). Since that time, it seems to be in bright state ($V \sim 14.6$–13.6). A first (extremely uncertain) estimate of its period by Chen et al. (2001) put it right in the middle of the period gap, with a period of 0.107 days, or 2.57 hr. However, a 45 day observation (Patterson 2002; Patterson et al. 2005b) corrected this value to 0.14923 days, or 3.58 hr, as expected for VY Scl stars, which usually have periods between ∼3 and ∼4 hr. BB Dor exhibits superhumps, with a period excess of $\varepsilon = 9.4\%$ (Patterson 2002); it has the largest known fractional superhump of all systems, and therefore provides a calibrating point at large ε (Patterson et al. 2005b). BB Dor is a VY Scl NL, and so far no magnetic activity has been found. The system also exhibits quasi-periodic oscillations (Chen et al. 2001). Chen et al. (2001) also noted that due to its very narrow Balmer lines (with wings extending ∼650 km s^{-1} from the line center), BB Dor is most likely a low-inclination system. From the Austral Variable Star Observer Network (AVSON), it appears that BB Dor has been around $V \approx 13.6$–14.6 mag (with an error <0.1 mag) for the last couple of years and can vary as much as 0.4 mag within 1 hr. The reddening value $E(B-V)$ toward BB Dor is not known. However, the Galactic reddening value in the direction of BB Dor as inferred from the 100 μm dust emission map (Schlegel et al. 1998) is very small: $E(B-V) = \sim 0.03$. Since the dust map gives the maximum dust extinction, we deduce that BB Dor must have a negligible reddening [$E(B-V) \sim 0.01$ at most], which should not affect the results; consequently we do not deredden its *FUSE* spectrum.

2. OBSERVATIONS

2.1. *The FUSE Spectrum of BB Dor*

BB Doradus was observed with *FUSE* on 2007 July 9 at 02:51:09 (UT), and three exposures were obtained (H9030301; exposures 001, 002, 003). The *FUSE* spectrum was obtained through the low-resolution (LWRS; $30'' \times 30''$) aperture in `TIME TAG` mode. The data were processed with the last and final version of CalFUSE, version 3.2.0 (Dixon et al. 2007).

A look at the count rate graph (generated by CalFUSE) indicates that the data for each exposure were collected mainly during the first 1000 s, followed by a jitter lasting about 1500 s. Toward the end of each exposure, the count rate dropped to zero. Therefore, while the coadded exposures for the 8 individual segments after processing by CalFUSE give a good exposure time (after screening) of between about 8750 s for segments SiC1a, SiC1b, LiF1a, and LiF1b (segments 1) and 9750 s for segments SiC2a, SiC2b, LiF2a, and LiF2b (segments 2), the count rate plot indicates that the total *good collection time* ranges between 3350 s (segments 1) and 3650 s (segments 2). We therefore weighted these segments accordingly, multiplying the flux (on the order of 1×10^{-13} erg s^{-1}cm $^{-2}$ Å^{-1} in the online preview) by a factor of 2.61 (segments 1) and 2.67 (segments 2). After that, we processed the data as usual (see below).

The spectral regions covered by the spectral channels overlap, and these overlap regions are then used to scale the spectra in the SiC1, SiC2, and LiF2 channels to the flux in the LiF1 channel. The low-sensitivity portions (usually the edges) of each channel are discarded. In the present case, the SiC2b spectral segment was very noisy, and we discarded it too. We also carried out a visual inspection of the *FUSE* channels to locate "the worm" (a wire flaw in the *FUSE* spectrograph that occults the saggital focus), and we manually discarded those portions of the spectrum affected by the worm. We combined the individual exposures and channels to create a time-averaged spectrum weighting the flux in each output datum by the exposure time and sensitivity of the input exposure and channel of origin. The final product is a spectrum that covers the full *FUSE* wavelength range of 905–1187 Å. Because we disregarded the right edge of both the SiC1a and SiC2b segments, there is a gap between the LiF1a and LiF2b segments (∼1082–∼1087 Å).

The *FUSE* spectrum of BB Dor is shown in Figure 1. Note that the *FUSE* exposures of BB Dor consist entirely of observations carried out during the day. The short night exposure was ignored because of jitters and other problems. We suspect that most of the emission lines are due to helio- and geocoronal emissions.

2.2. *The FUSE Lines*

The *FUSE* spectra of CVs exhibit mainly broad absorption lines from the accretion disk and WD, as well as sharp absorption lines from circumstellar (or circumbinary) material and the interstellar medium (ISM). Emission lines from the hotter regions are usually broadened, depending on the inclination angle i, due to the large Keplerian velocity in the inner disk. Sharp emission lines from air glow (geo- and heliocoronal in origin) are also present, due mainly to the reverberation of sunlight inside the *FUSE* telescope during daytime observations. The present *FUSE* spectrum of BB Dor presents such a complexity, and all the lines are listed in Table 1.

Absorption lines.— The main characteristic of the *FUSE* spectrum of BB Dor is the broad Lyβ absorption feature due to either the exposed WD, the disk at low inclination angle i, or possibly both (see § 4). Absorption features from the higher orders of the Lyman series are also clearly visible, indicating a

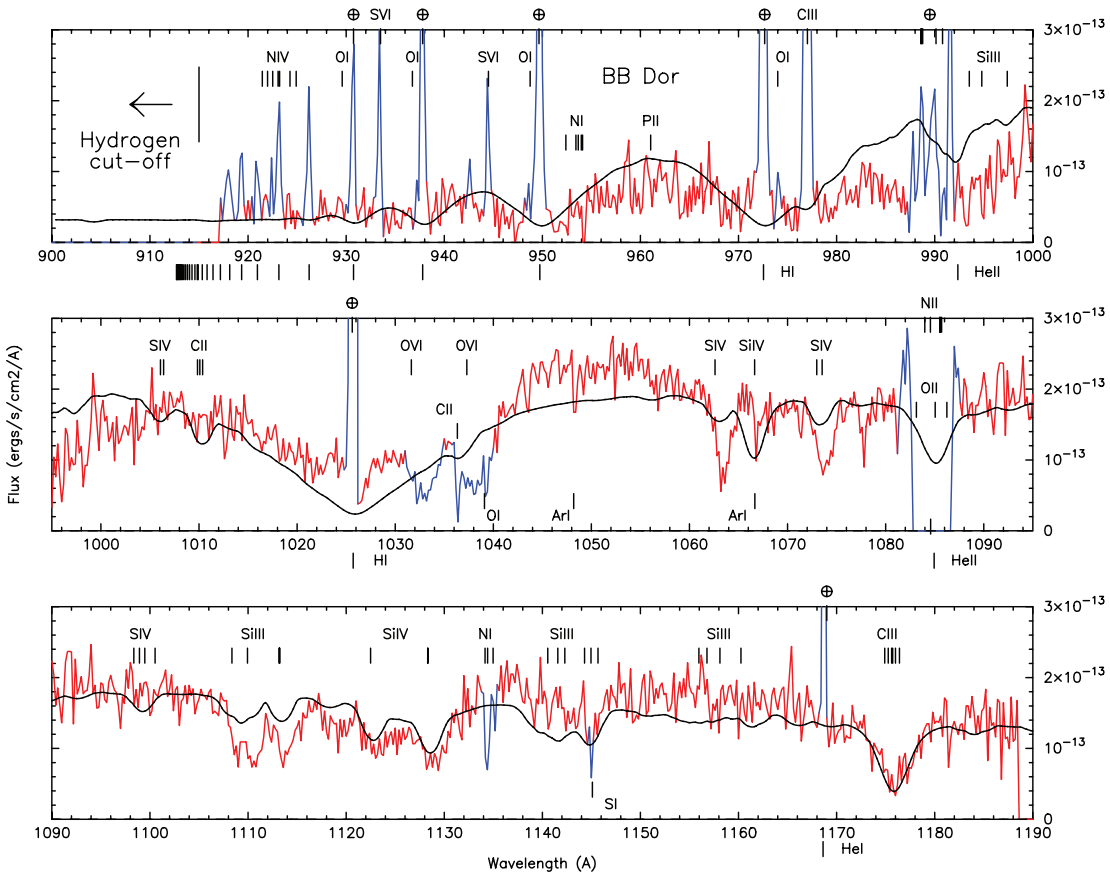

FIG. 1.— Solar abundance, single-WD model. The best-fit WD model assuming solar abundances (*solid black line*) is shown together with the *FUSE* spectrum of BB Dor (*red line*). Blue lines show the segments of the spectrum that were masked before the fitting. The WD has a temperature $T = 37{,}000$ K, a projected rotational velocity $V_{\rm rot} \sin i = 400$ km s^{-1}, and $\log g = 8.3$. The distance obtained is $d = 217$ pc, and $\chi^2_\nu = 0.3348$.

temperature $T \sim 35{,}000$ K. The other main absorption features expected at this temperature are C III (1175 Å), Si III (≈1108–1114 Å and ≈1140–1144 Å), Si IV (≈1120–1130 Å), and C II (1010 Å). The spectrum is, however, also marked by some high-order ionization absorption lines, such as S IV (1063 and 1073 Å), Si IV (1066.6 Å), and the O VI doublet. The S IV (1006 Å), C II (1010 Å), and S IV (1099 Å) absorption multiplets are all unresolved and shallow. However, we have indicated them on the figures, as they appear deeper in the modeling. On the other hand, the S IV (1063 and 1073 Å) and Si III (∼1010 Å) absorption lines appear deeper in the observed spectrum than in the modeling. The presence of high-order ionization species (such as the oxygen doublet) indicates the presence of a hotter absorbing component above the main FUV-emitting region. The P II line (∼961 Å) has been marked in the spectrum, although the feature is most probably due to noise. All the lines are listed in Table 1 with their wavelengths. Most of the broad absorption lines and features associated with the source are redshifted by about 0.6–0.9 Å, corresponding to a receding velocity of 200 ± 40 km s^{-1}. It seems very likely that this redshift is due to the orbital motion of the WD; however, we do not have enough time tag data to verify this assumption.

Emission lines.— The spectrum of BB Dor exhibits sharp emission lines, including all the orders of the Lyman series, N IV (∼923 Å), S VI (933.5 and 944.5 Å), C III (977 Å), He II (992 Å), and He I (1068 Å). Some of these lines, in particular the H I lines, the He I and He II lines, the C III (977 Å) line, and the O VI doublet, seem to be due to heliocoronal emission (sunlight reflected inside the telescope), which contaminates the SiC channels. The segments of the spectrum from the LiF channels overlapping the SiC Channels down to about 1000 Å do not show any oxygen lines, and we therefore did not include these spectral regions of the SiC channels. However, other emission lines may be solely from the source. In many NLs, the emission lines from the disk are broadened by the Keplerian velocity and are consequently easily identified. However, Chen et al. (2001) have detected very narrow Balmer lines and concluded that BB Dor is most likely a low-inclination system. Because of this, the identification of the emission lines from the source is not trivial. This issue is further complicated by the lack of night exposure and the very low signal-to-noise ratio, which makes it difficult to analyze the two-dimensional image of the spectrum for the effect of scattered sunlight on the emission lines.

Since the system is a NL in a high state, we first expect the N IV (≈923 Å), S VI (933.5 and 944.5 Å), and C III (977 Å) emission lines to be from the source, with some possible heliocoronal contamination mostly affecting the carbon emission lines. The N IV (923.06 Å) emission line is contaminated with the H I (923.15 Å) line, while the N IV (922.52 and 924.28 Å) lines are not. However, the complete absence of narrow emission lines from the oxygen doublet and C III (1175 Å) seems to indicate otherwise; i.e., all the sharp emission lines might be heliocoronal in origin. To further check this possibility, we measured the relative intensities of the narrow emission lines below 1000 Å and compared them with those of the solar spectrum (Curdt et al. 2001). We found good agreement with the solar disk–average quiet-Sun data, except for S VI (944.5 Å), which has a higher relative intensity in the spectrum of BB Dor. This could be due to sunspot activity during the *FUSE* observation of BB Dor, as this line intensity increases by a factor of 30 inside sunspots, while the other lines increase

TABLE 1
FUSE Line Identification

Ion	λ_{rest} (Å)	λ_{obs} (Å)	Origin/Nature of Line[a]
H I	918.13	918.0	c/e
	919.35	919.3	c/e
	920.96	920.9	c/e
N IV	922.52	922.3	s/e
	923.06	923.0	s, c/e
H I	923.15	923.2	c/e
N IV	923.22	923.2	c/e
	924.28	924.2	c/e
H I	926.23	926.2	c/e
	930.75	930.7	c/e
S VI	933.50	933.4	c/e
H I	937.80	937.8	c/e
S VI	944.50	944.4	c/e
H I	949.74	949.7	c/e
N I	952.40	925.5	ism/a
	953.42	...	...
	953.66	...	...
	953.97	...	...
	954.10	954.2	ism/a
P II	961.04	961.2	ism/a?
H I	972.54	972.5	c/e
C III	977.02	977.0	c/e
Si III	993.52	993.2	s?/a
	994.19	994.9	s?/a
	997.39	997.1	s?/a
S IV	1006.07	...	s/a - unresolved
	1006.39	...	s/a - unresolved
C II	1009.85	...	s/a - unresolved
	1010.08	...	s/a - unresolved
	1010.37	...	s/a - unresolved
H I	1025.77	1025.7	c/e
O VI	1031.91	1032.9	s/a
C II	1036.34	1036.4	ism/a
O VI	1037.61	1038.3	s/a
O I	1039.10	1039.3	ism/a
Ar I	1048.20	1048.3	ism/a
S IV	1062.65	1063.4	s/a
Si IV	1066.60	1067.1	s/a
Ar I	1066.66	1066.8	ism/a
S IV	1072.97	1073.9	s/a
	1073.52	1073.9	s/a
S IV	1098.36	...	s/a - unresolved
	1098.93	...	s/a - unresolved
	1099.48	...	s/a - unresolved
	1100.53	...	s/a - unresolved
Si III	1108.36	1108.8	s/a
	1109.94	1110.6	s/a
	~1113.20	1113.8	s/a
Si IV	1122.49	1123.0	s/a
	~1128.33	1128.9	s/a
N I	1134.16	1134.3	c/a
	1134.42	1134.3	c/a
	1134.98	1135.2	c/a
S I	1145.10	1145.0	ism/a
He II	1168.61	1168.6	c/e
C III	1174.90	1176.4	s/a - unresolved
	1175.26	1176.4	s/a - unresolved
	1175.60	1176.4	s/a - unresolved
	1175.71	1176.4	s/a - unresolved
	1176.00	1176.4	s/a - unresolved
	1176.40	1176.4	s/a - unresolved

[a] (a): absorption; (e): emission; (c): contamination (e.g., air glow; heliocoronal emission); (s): source; "ism"indicates interstellar medium.

by at most a factor of 3. We therefore conclude that all the sharp emission lines in the *FUSE* spectrum of BB Dor are due to sunlight reflected inside the telescope.

3. SPECTRAL MODELING

We created a grid of models of synthetic spectra of WDs and accretion disks for different values of the WD temperature $T_{\rm eff}$, gravity log g, projected rotational velocity $V_{\rm rot}$ sin i, inclination i, mass accretion rate $\dot{M}$, and abundances. We then ran a χ^2 fitting program to find the best fit for (1) a single WD component, (2) a single accretion disk component, and (3) a combined WD+accretion disk. We describe below how we generate these synthetic spectra and how we perform the fitting.

We create the synthetic model spectra for high-gravity stellar atmospheres using the TLUSTY and SYNSPEC[3] codes (Hubeny 1988; Hubeny & Lanz 1995). Atmospheric structure is computed (using TLUSTY) assuming a H-He LTE atmosphere; the other species are then added in the spectrum synthesis stage using SYNSPEC. We generate photospheric models with effective temperatures ranging from ~20,000–50,000 K in increments of 1000 K. We chose values of log g ranging between 7.5 and 9.0. We also varied the stellar rotational velocity $V_{\rm rot}$ sin i from 100 to 1000 km s^{-1} in steps of 100 km s^{-1} (or smaller if needed). The WD rotation ($V_{\rm rot}$ sin i) rate is determined by fitting the WD model to the spectrum while paying careful attention to the line profiles in the *FUSE* spectrum. We do not carry out separate fits to individual lines, but rather try to fit the lines and continuum simultaneously, while paying careful attention to the absorption lines. It is important to note that the depth of the absorption features depends not only on the abundances, but also on the rotational velocity. Increasing the rotational velocity reduces the central depths of the absorption features, thus reducing the abundance. However, the widths of the absorption features also increase with increasing rotational velocity. As a consequence, abundances and rotational velocity effects are intertwined, and cannot always be easily separated without additional information about one of the parameters. For any WD mass, there is a corresponding radius, or equivalently one single value of log g (e.g., see the mass radius relation from Hamada & Salpeter [1961], or see Wood [1990] or Panei et al. [2000] for WDs of different compositions and nonzero temperature). Therefore, by scaling the theoretical spectrum to the observed one, we obtain the distance to the system.

We model accretion disk spectra by first assuming that the disk is made of a collection of annuli, where each annulus has a temperature $T(r)$ and gravity log $g(r)$, as given by the standard disk model (Shakura & Sunyaev 1973; Pringle 1981), for a given central mass $M_{\rm WD}$ and accretion rate $\dot{M}$. A variant of the TLUSTY code, called TLDISK, is then used, which generates an atmosphere model for each annulus that is then used as input for SYNSPEC. The contribution of all the annuli are then combined using DISKSYN, and a final spectrum is obtained for any given inclination angle. A detailed explanation of the procedure is given in Wade & Hubeny (1998). In the present work, we do not use the grid of synthetic accretion disk spectra tabulated by Wade & Hubeny (1998); instead, we generate them. This allows us to compute disk spectra assuming nonsolar abundances and for any inclination angle (the disk spectra of Wade & Hubeny [1998] have solar abundances and have been generated for a specific value of the inclination i).

Before carrying out a synthetic spectral fit of the spectra, we masked portions of the spectra with strong emission lines, strong

[3] TLUSTY, ver. 200 and SYNSPEC, ver. 48; see http://nova.astro.umd.edu.

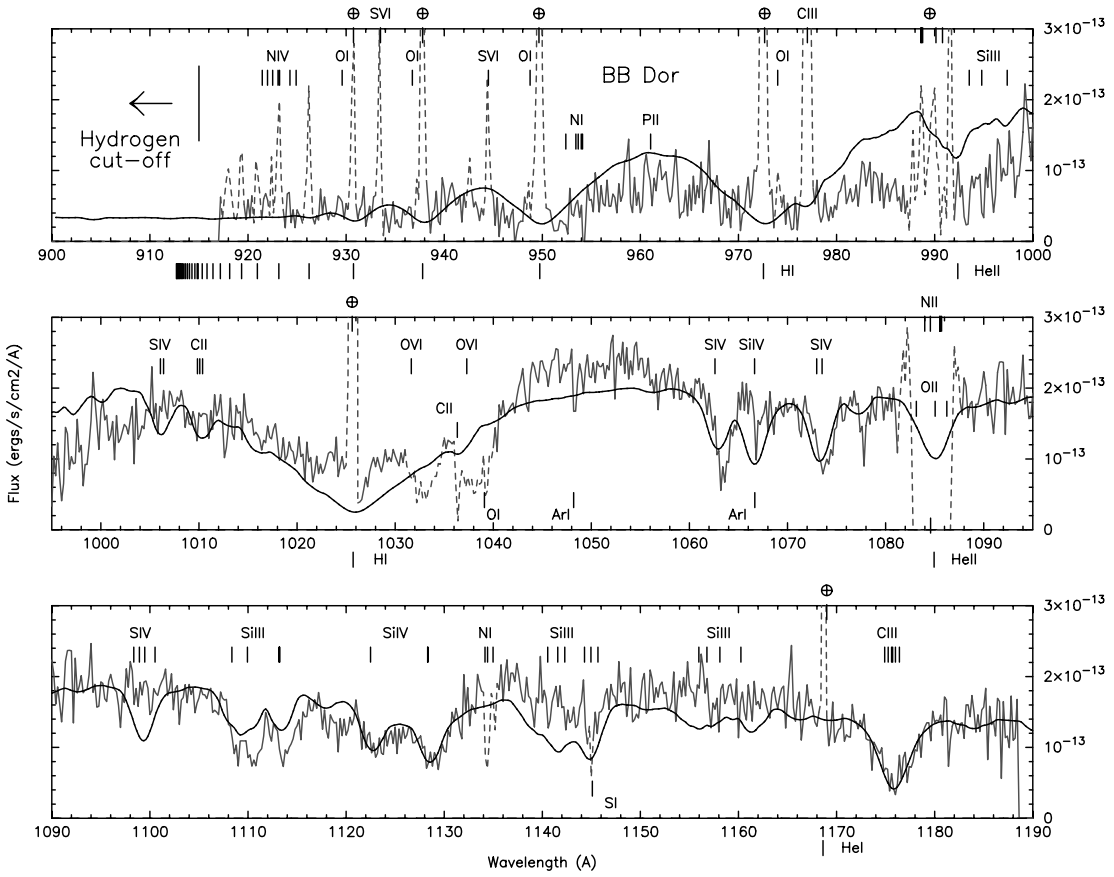

FIG. 2.—Nonsolar abundance, single-WD model. The best-fit WD model (*solid black line*) to the *FUSE* spectrum of BB Dor (*solid gray line*) is shown, where the abundances of sulfur and silicon have been set to [S] = 20 solar and [Si] = 3 solar. The abundances of all the other elements have been set to solar. Dashed gray line segments show the segments of the spectrum that were masked before the fitting. The WD has a temperature $T = 37{,}000$ K, a projected rotational velocity $V_{\rm rot} \sin i = 400$ km s^{-1}, and $\log g = 8.3$. The distance obtained is $d = 211$ pc, and $\chi^2_\nu = 0.3129$. [*See the electronic edition of the Journal for a color version of this figure.*]

ISM absorption lines, detector noise, and air glow. The regions excluded from the fit appear in blue in Figure 1.

After generating grids of models for the *FUSE* spectrum of BB Dor, we use FIT (Press et al. 1992), a χ^2 minimization routine, to compute the reduced χ^2_ν (i.e., χ^2 per number of degrees of freedom) and scale factor (which gives the distance) for each model fit. While we use a χ^2 minimization technique, we do not blindly select the least-χ^2 models, but we also examine the models that best fit some of the features such as absorption lines and, when possible, the slope of the wings of the broad Lyman absorption features.

Initially, we generate solar abundance models, and when a good fit is found, we start varying the chemical abundances of C, N, S, and Si to fit the absorption features of the spectrum. In particular, the carbon abundance was set using the C II (1010 Å) and C III (1175 Å) multiplets, the sulfur abundance was set using the S IV (1063 and 1073 Å) lines, and the silicon abundance was set using the Si IV (1067 , 1023 , and 1028 Å) and Si III (∼1110 and ≈1138–1146 Å) lines.

4. RESULTS

The data obtained by AVSON imply that BB Dor has been in a high state around $V \approx 13.6$–14.6 for the last couple of years. We therefore expect the *FUSE* spectrum to be dominated by flux from the accretion disk with a relatively high $\dot{M}$. However, in our modeling we follow a systematic approach that consists of fitting (1) a single WD, (2) a single accretion disk, and (3) a WD+accretion disk composite.

4.1. *White Dwarf*

Since we do not have any information about the mass of the WD, we look for all the best-fit models in the $\log g$-$T_{\rm eff}$ plane. Namely, for each assumed value of $\log g$, we vary the temperature to find the best-fit model. As expected, we find that the temperature is somewhere between 34,000 K (for $\log g = 7.5$) and 40,000 K (for $\log g = 9.0$), with a distance between 377 and 135 pc, respectively (see Table 1). The least χ^2_ν is obtained for $\log g = 8.0$–8.65. We chose the intermediate-value $\log g = 8.3$ model, with $T = 37{,}000$ K, $d = 247$ pc, and solar abundances to illustrate our results in Figure 1. We then further improve the fit by varying the abundances. We find that in order to better fit the sulfur and silicon lines, we have to set the sulfur to 20 times its solar abundance, and the silicon to 3 times, while all the other species are kept at solar abundances. The χ^2_ν value decreases from 0.3348 to 0.3129 (by about 7%). While some of the lines are better fitted (such as S IV 1063 and 1073 Å, Si III ∼1010 Å, and Si IV ∼1025 Å), the S IV (1006 and 1100 Å) are far too deep (see Fig. 2).

4.2. *Accretion Disk*

Next, we fit the solar abundance disk models. We find that a low inclination is needed in order to match the absorption lines, and in our models we initially set $i = 5°$, $8°$, $12°$, and $18°$. Again, because we have no information about the mass of the WD, for each value of $\log g$ (ranging between 7.5 and 9.0) we vary the mass accretion rate between $10^{-10.5}$ and $10^{-8.0}$ $M_\odot$ yr^{-1} to find the best-fit models. Again, we find that the best-fit models are

TABLE 2
SYNTHETIC SPECTRA

log g (cgs)	T_{WD} (10^3 K)	$V_{rot} \sin i$ (km s^{-1})	[Si] (solar)	[S] (solar)	[Z] (solar)	i (deg)	log$\dot{M}$ ($M_\odot$ yr^{-1})	WD/Disk (%)	d (pc)	χ^2_ν	Figure
7.50.....	34.0	400	1.0	1.0	1.0	...	...	100/0	377	0.3427	
8.00.....	36.0	400	1.0	1.0	1.0	...	...	100/0	266	0.3361	
8.30.....	37.0	400	1.0	1.0	1.0	...	...	100/0	247	0.3348	1
8.30.....	37.0	400	3.0	20.	1.0	...	...	100/0	211	0.3129	2
8.50.....	38.0	400	1.0	1.0	1.0	...	...	100/0	193	0.3345	
8.50.....	38.0	400	3.0	20.	1.0	...	...	100/0	184	0.3100	
8.65.....	38.0	400	1.0	1.0	1.0	...	...	100/0	172	0.3360	
9.00.....	40.0	400	1.0	1.0	1.0	...	...	100/0	135	0.3390	
7.50.....	...	...	1.0	1.0	1.0	12	−8.0	0/100	878	0.3346	
7.88.....	...	...	1.0	1.0	1.0	12	−8.5	0/100	878	0.3346	
8.30.....	...	...	1.0	1.0	1.0	8	−9.0	0/100	693	0.3297	
8.30.....	...	...	3.0	20.	1.0	8	−9.0	0/100	665	0.3000	3
8.65.....	...	...	1.0	1.0	1.0	5	−9.5	0/100	496	0.3332	
9.00.....	...	...	1.0	1.0	1.0	5	−10.0	0/100	361	0.3376	
8.30.....	32.0	400	3.0	20.	1.0	08	−9.0	10/90	700	0.2989	4
8.30.....	37.0	400	3.0	20.	1.0	80	−9.0	74/26	246	0.2873	5
8.65.....	38.0	400	3.0	20.	1.0	80	−9.5	75/25	184	0.2880	

around log $g = 8.3$, but the difference between the χ^2_ν values is not significant, and the improvement over the single-WD models is also only marginal (on the order of ∼1% in the χ^2_ν value). All these models are presented in Table 2. Next, we improve the disk model by varying the abundances, although we do not expect the fit to improve much because of the Keplerian velocity broadening of the disk. However, we find that setting the silicon and sulfur abundances to 3 and 20 times solar, respectively, actually reduces the χ^2_ν value by 10%, which is more than for the single-WD model. This is because the S IV (1006 and

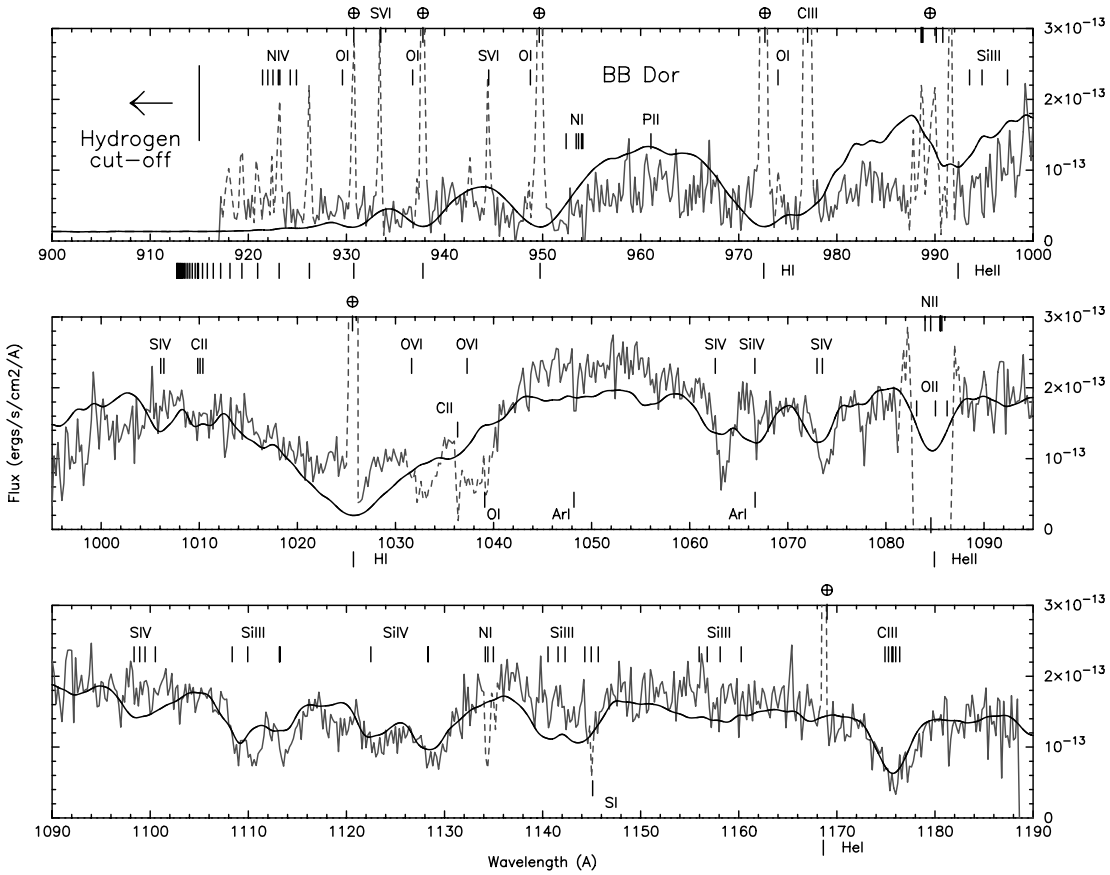

FIG. 3.—Nonsolar abundance, single-disk model. The *FUSE* spectrum of BB Dor is shown together with one of the best-fit synthetic disk models (*solid black line*). The model has $M = 0.80\,M_\odot$, $\dot{M} = 10^{-9}\,M_\odot$ yr^{-1}, $i = 8°$, a distance $d = 665$ pc, and $\chi^2_\nu = 0.3000$. Abundances and solid gray/dashed gray spectral segments are as in Fig. 2. The low inclination is needed in order to fit the silicon, sulfur, and carbon absorption lines. [*See the electronic edition of the Journal for a color version of this figure*.]

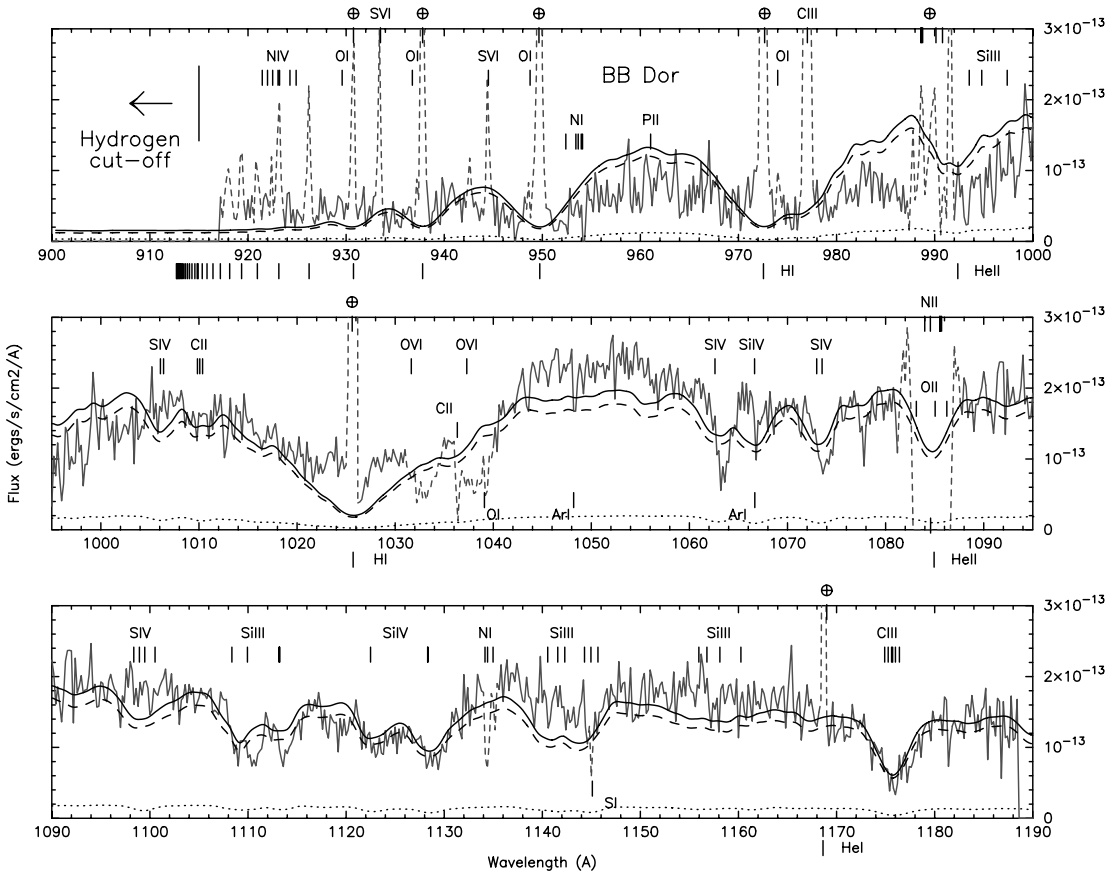

FIG. 4.—Low-inclination, nonsolar abundance, WD+disk model. The *FUSE* spectrum of BB Dor is shown together with one of the best-fit WD+disk models (*solid black line*), assuming a low inclination angle. The model has $M = 0.80\,M_{\odot}$, $\dot{M} = 10^{-9}\,M_{\odot}$ yr^{-1}, $i = 8^{\circ}$, a distance $d = 700$ pc, and $\chi^2_{\nu} = 0.2889$. Abundances and solid gray/dashed gray spectral segments are as in Fig. 2. The WD (*dotted line*) contributes 10% of the flux, while the high-inclination disk (*dashed black line*) contributes the remaining 90%. [*See the electronic edition of the Journal for a color version of this figure.*]

1100 Å) lines have better fits (Fig. 3). This best-fit single-disk model has $i = 8^{\circ}$, $\dot{M} = 10^{-9}\ M_{\odot}$ yr^{-1}, a distance of 665 pc, and $\chi^2_{\nu} = 0.3000$.

4.3. *Composite Model: WD+Accretion Disk*

Last, we fit composite WD+Disk models. Since the number of models increases exponentially when we change log g, $T_{\rm eff}$, and $\dot{M}$, we restrict our search using our best fit for log g, namely 8.3. We also set the sulfur to 20 times solar and silicon 3 times solar. This procedure reduces the number of free parameters to 3 ($\dot{M}$, $T_{\rm eff}$, i).

Low inclination.— Since the system is believed to have a low inclination angle (Chen et al. 2001), we generate low-inclination models ($i = 5^{\circ}$, 8°, 12°, and 18°). Not surprisingly, the best fit model has $i = 8^{\circ}$ and $\dot{M} = 10^{-9}\ M_{\odot}$ yr^{-1}, but this time the WD has a temperature of 32,000 K and provides only 10% of the flux, while the disk provides the remaining 90%. Such a model again brings an insignificant improvement in the value of χ^2_{ν}, and it is clear (Fig. 4) that it is barely distinguishable from the best-fit single-disk model. From the point of view of the physics, this model is preferred because, if the system has a low inclination angle, then the emission from the WD must contribute to the flux. Models with a WD temperature $T < 30{,}000$ K have a WD contribution of only a few percent of the total FUV flux, and cannot be distinguished from the single-disk models. If the WD has a temperature $T_{\rm eff} < 30{,}000$ K, it will not be detected while the system is in a high state (with $\dot{M} = 10^{-9}\,M_{\odot}$ yr^{-1}). These results imply that the contribution from the WD is not very large and that the temperature of the WD must be $\leq$32,000 K.

High inclination.— From the sharp Balmer emission lines, Chen et al. (2001) suggest that the system has a low inclination. However, we cannot confirm the inclination directly from the emission lines of the *FUSE* spectrum, as *all* the sharp emission lines in the *FUSE* spectrum are of heliocoronal origin. Our low-inclination, single-disk models provide a slightly better fit than the single-WD models (and a much better fit than the high-inclination, single-disk models); however, for completeness we include here the results from the composite WD+disk model fits when the assumption about the inclination angle is relaxed.

We search for the best-fit WD+disk models (assuming log g = 8.3) in the $T_{\rm eff}$-$\dot{M}$ parameter space using *all* inclination angles, and find that the models with an intermediate inclination (i = 18°, 41°, 60°, and 75°) do not provide the best fit. The best-fit model has $i = 80^{\circ}$ and reflects a situation in which the WD is dominant with $T = 37{,}000$ K and contributes 3/4 of the total flux, while the disk has $\dot{M} = 10^{-9} M_{\odot}$ yr^{-1} and contributes only 1/4 of the flux. The distance obtained from this model is 246 pc and $\chi^2_{\nu} = 0.2873$. This is the least χ^2 value we obtained from all our models. This model is presented in Figure 5. Similar results were obtained assuming log $g = 8.65$, but with a slightly lower mass accretion rate (Table 2).

5. DISCUSSION AND CONCLUSION

BB Dor is a little-known southern NL, and consequently both the distance and the mass of the WD are unknown, which implies a larger uncertainty in the results. In addition, the *FUSE* spectrum is definitely of poor quality. In theory, a fine-tuning of the temperature (say to an accuracy of about $\pm$50 K) and mass

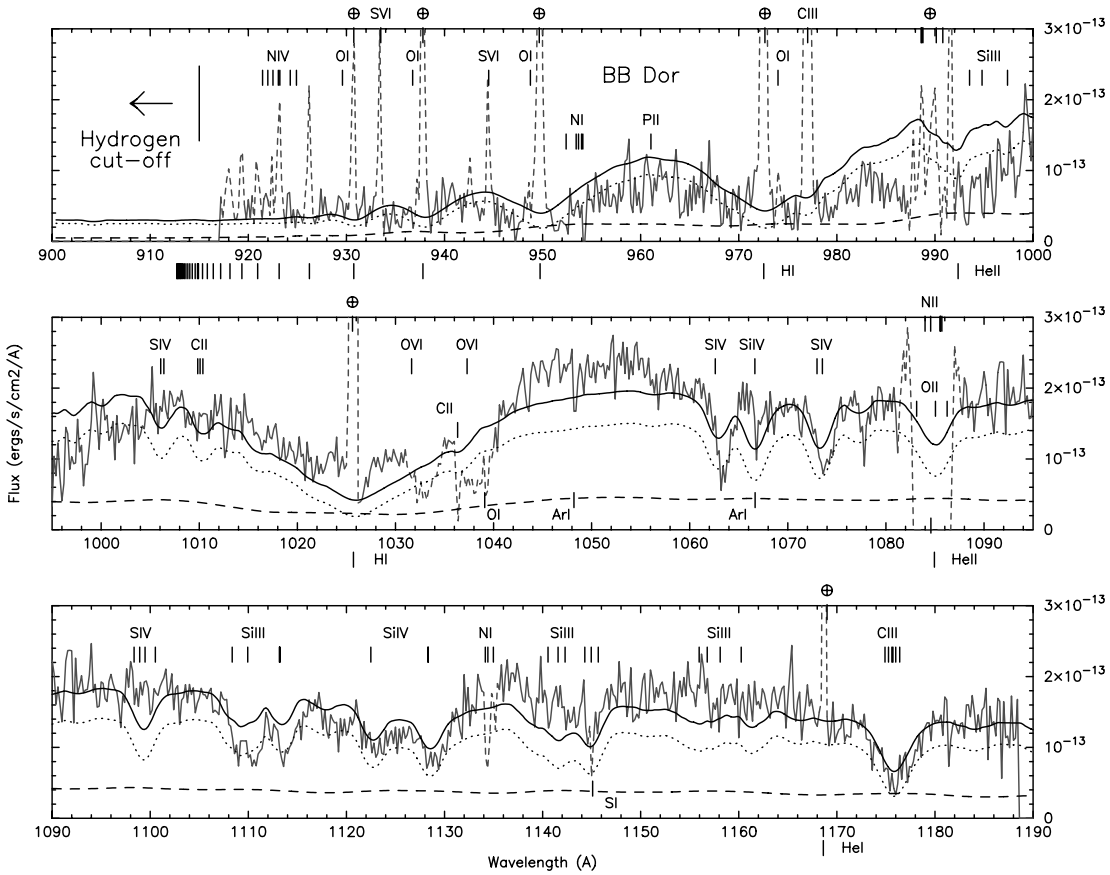

FIG. 5.—High-inclination, nonsolar abundance, WD+disk model. The *FUSE* spectrum of BB Dor is shown together with one of the best-fit WD+disk models (*solid black line*). The model has $M = 0.80\ M_{\odot}$, $\dot{M} = 10^{-9}\ M_{\odot}\ \mathrm{yr}^{-1}$, a distance of $d = 246$ pc, and $\chi^2_{\nu} = 0.2873$. The inclination angle of the system is kept as a free parameter, and the best-fit model gives $i = 80^{\circ}$. Abundances and solid gray/dashed gray spectral segments are as in Fig. 2. The fits of the silicon, sulfur, and carbon absorption lines are obtained by letting the WD component dominate the spectrum. The WD (*dotted line*) contributes 74% of the flux, while the high-inclination disk (*dashed black line*) contributes the remaining 26%. [*See the electronic edition of the Journal for a color version of this figure.*]

accretion rate can be carried out by fitting the flux levels, such that the distance to the system (when known) is obtained accurately. However, the fitting to the distance depends strongly on the radius (and therefore the mass) of the WD. We discuss below some additional restrictions that we use to constrain the properties of the system.

On the basis of the least χ^2_{ν}, the best model is the high-inclination, WD+disk composite. However (see Fig. 5), because of the high inclination, the disk contributes a rather flat component all the way into the shorter wavelengths. At such a high inclination, one would not expect the WD to dominate the flux, but rather the WD would be almost completely masked by the swollen disk; actually, the system would likely be observed to undergo eclipses, but none have been observed. Also, since BB Dor can vary as much 0.4 mag in 1 hr, this means that the light cannot be dominated by the WD, and that the disk must be contributing at least 40% of the light. In other words, while the least χ^2 indicates that the best fit is a WD with a rather flat disk component, there are other indications that this cannot be correct. Actually, the WD+disk, high-inclination model strikingly resembles the second component observed in the *FUSE* spectra of some dwarf novae during quiescence (e.g., VW Hyi; Godon et al. 2004). This is likely a caveat in state-of-the-art spectral modeling rather than an indication of a physical link between the spectrum of BB Dor and that of a DN in quiescence. The need for improved modeling also stems from the difficulty in producing a model that fits low- and high-order ionization lines at the same time. For BB Dor, it is possible that the S IV 1063 and 1073 Å absorption lines form in the same hotter region/layer where the O VI doublet forms, while the C III and Si III lines form in a cooler region/layer where the Lyman series (and continuum) form. This is similar to the *Hubble Space Telescope* STIS spectrum of TT Crt (Sion et al. 2008), which exhibits a rich variety of absorption lines from different ionization stages, suggesting line formation in (at least) two different temperature regions.

In order to reduce the size of the domain for which we have best-fit models in the parameter space, we use the infrared magnitudes J, H, and K from the Two Micron All Sky Survey (2MASS) to assess the distance to BB Dor as prescribed by Knigge (2006) for systems with $P < 6$ hr. The IR data were collected on 1999 November 9, at a time when BB Dor was in a high state with a visual red magnitude $R = 14.60$ and a blue magnitude $B = 13.90$ (whereas $B \sim 16.5$ in the low state). The 2MASS IR apparent magnitudes are $J = 14.322$, $H = 14.089$, and $K = 14.053$. For a primary star with $M_{\mathrm{WD}} = 0.75\ M_{\odot}$ and period of 3.559 hr (corresponding to BB Dor), the donor star mass is $M_2 = 0.25\ M_{\odot}$ (Patterson et al. 2005b suggest $M_2 = 0.256\ M_{\odot}$), and the IR absolute magnitude estimates are $M_J = 7.47$, $M_H = 6.90$, and $M_K = 6.63$. Inserting these into equation (15) of Knigge (2006) gives distances of 235, 274, and 305 pc, respectively. These distances are typically underestimated by factors of 2.05, 1.86, and 1.75 for the J, H and and K bands, giving distances of 482, 510, and 534 pc, respectively, assuming that the donor star contributes only ~1/4–1/3 of the total IR flux (Knigge 2006).

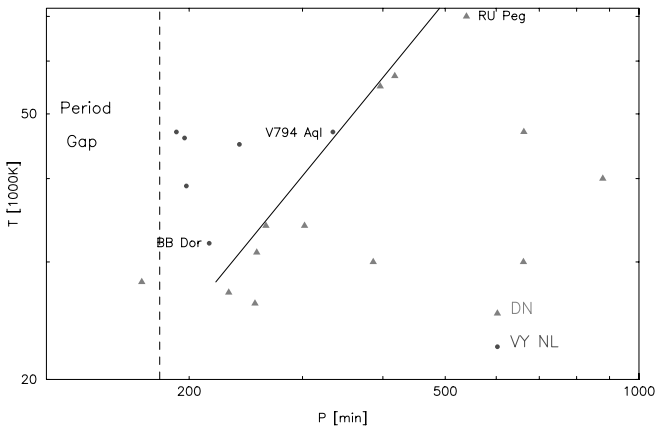

FIG. 6.— Dwarf nova systems and VY Scl NLs above the period gap. The systems are plotted in the ($T_{\rm eff}$, P) parameter space on a logarithmic scale. The data for the NLs are taken from Hamilton & Sion (2008) and references therein. The data for the dwarf nova systems are taken from Sion et al. (2008) and references therein. For RU Peg, we have used the more recent estimate from Godon et al. (2008). The data point for V794 Aql is an estimate of the WD temperature based on an IUE spectrum while the system was in a lower state (Godon et al. 2007). While the data point of BB Dor is lower than those of the other VY Scl systems, there is still a clear separation between the VY Scl systems and the DN systems, as indicated by the slanted line. [*See the electronic edition of the Journal for a color version of this figure*.]

The distance to BB Dor is therefore certainly larger than 300 pc, and most likely in the range of ~500 pc. Since BB Dor was observed in a high state (with 2MASS), it is likely that the infrared flux of the donor star is on the lower side, namely even less than 1/4, in which case the 500 pc itself is only a lower limit. Using this restriction on the distance, we can safely reject the single-WD models (with $d < 400$ pc), the high-inclination models (with $d < 250$ pc), and the large-mass $\log g = 9.0$ models (with $d = 361$ pc or less).

On the basis of the distance alone, the low-inclination disk and WD+disk models are the best fits. These are also the best fits on the basis of the optical spectrum (low inclination) and visual magnitude (high state/disk).

We are now able to summarize the basic characteristics of the system and its WD. We are confident that the system must have a WD with $\log g = 8.3 \pm 0.3$, $T_{\rm eff} = 32{,}000$ K *or lower* (disk+WD composite models), a mass accretion rate on the order of $\dot{M} = 10^{-9}\ M_{\odot}\ {\rm yr}^{-1}$ (disk and disk+WD models), and a distance somewhere between 500 and 700 pc (choosing the least χ^2 models agreeing with the distance). From the best-fit single-disk models alone, we find that the inclination angle must be very small (~8°) to fit the absorption lines. There is an indication that the sulfur and silicon are overabundant, and it is also possible that some of the high-order ionization lines form in a layer in front of the disk and the WD.

Although the *FUSE* spectrum of BB Dor is rather poor, and multiwavelength data are limited, we have narrowed down the region in the parameter space ($\dot{M}$, P, $T_{\rm eff}$) for this system. BB Dor is now the sixth VY Scl NL variable with a temperature estimate for its WD. With a temperature of $\leq$32,000 K, the WD of BB Dor marks the lower end of the temperature distribution for WDs of VY Scl NL variables, which, so far, for the other five systems, ranged between 40,000 and 47,000 K (Hamilton & Sion 2008). The *FUSE* spectrum of BB Dor clearly shows the drop in flux in the shorter wavelengths, which is the signature of a moderate temperature when compared to the *FUSE* spectra of the other VY Scl systems (see e.g., V794 Aql; Godon et al. 2007). Even if we consider the best-fit single-WD model, the WD temperature of BB Dor only reaches 37,000 K (the model with 40,000 K and $\log g = 9.0$ gives an unrealistically close distance of 135 pc, in disagreement with the expected IR emission from the secondary). In that respect, the data point in the ($T_{\rm eff}$, P) plane for BB Dor falls *under* the region of the VY Scl NL variables, seemingly into the region of the parameter space populated with dwarf novae (Sion et al. 2008). However, as shown in Figure 6, the data point for BB Dor does not seem to stand apart, and the separation between VY Scl systems and DNs can be made easily by drawing a diagonal line. In that respect, it is actually V794 Aql that divides the two regions of the graph, as indicated by the slanted line.

We thank the anonymous referee for a prompt, concise, and pertinent report, which helped improve the analysis of the lines. Special thanks go to the Austral Variable Star Observer Network (AVSON), and in particular to Berto Monard for providing us with the visual magnitude of BB Dor between 2005 September 2 and 2007 December 30, as well as to Peter Nelson for quick-look V-band photometry of BB Dor on 2008 January 28. P. G. wishes to thank Mario Livio for his kind hospitality at the Space Telescope Science Institute, where part of this work was done. The infrared J, H, and K magnitudes of BB Dor were retrieved from the online archival data of the Two Micron All Sky Survey (2MASS) at the Infrared Processing and Analysis Center (IPAC). Part of this publication makes use of the data products from 2MASS, which is a joint project of the University of Massachusetts and IPAC at the California Institute of Technology, and is funded by NASA and the National Science Foundation. This research was based on observations made with the NASA-CNES-CSA *Far Ultraviolet Spectroscopic Explorer* (*FUSE*). *FUSE* is operated for NASA by the Johns Hopkins University under NASA contract NAS5-32985. This research was supported by NASA *FUSE* grant NNX07AU50G to Villanova University (P. G.). This work was also supported in part by NSF grant AST05-07514 to Villanova (E. M. S.).

REFERENCES

Andronov, N., Pinsonneault, M., & Sills, A. 2003, ApJ, 582, 358
Chen, A., O'Donoghue, D., Stobie, R. S., Kilkenny, D., & Warner, B. 2001, MNRAS, 325, 89
Curdt, W., Brekke, P., Feldman, U., Wilhelm, K., Dwivedi, B. N., Schüle, U., & Lemaire, P. 2001, A&A, 375, 591
Dixon, W. V., et al. 2007, PASP, 119, 527
Godon, P., Sion, E. M., Barrett, P. E., Hubeny, I., Linnell, A. P., & Szkody, P. 2008, ApJ, 679, 1447
Godon, P., Sion, E. M., Barrett, P. E., & Szkody, P. 2007, ApJ, 656, 1092
Godon, P., Sion, E. M., Cheng, F. H., Szkody, P., Long, K. S., & Froning, C. S. 2004, ApJ, 612, 429
Hamada, T., & Salpeter, E. E. 1961, ApJ, 134, 683
Hamilton, R. T., & Sion, E. M. 2008, PASP, 120, 165
Howell, S., Nelson, L, & Rappaport, S. 2001, ApJ, 550, 897
Hubeny, I. 1988, Comput. Phys. Commun., 52, 103
Hubeny, I., & Lanz, T. 1995, ApJ, 439, 875
Knigge, C. 2006, MNRAS, 373, 484
Panei, J. A., Althaus, L. G., & Benvenuto, O. G. 2000, A&A, 353, 970
Patterson, J. 2002, Center for Backyard Astrophysics (New York: CBA), http://cbastro.org/communications/news/2002/november21-a.html
Patterson, J., Thorstensen, J. R., & Kemp, J. 2005a, PASP, 117, 427
Patterson, J., et al. 2005b, PASP, 117, 1204
Press, W. H., Teukolsky, S. A., Vetterling, W. T., & Flannery, B. P. 1992, Numerical Recipes in Fortran, The Art of Scientific Computing (2nd ed.; Cambridge: Cambridge Univ. Press)
Pringle, J. E. 1981, ARA&A, 19, 137

Schlegel, D. J., Finkbeiner, D. P., & Davis, M. 1998, ApJ, 500, 525
Shakura, N. I., & Sunyaev, R. A. 1973, A&A, 24, 337
Sion, E. M. 1995, ApJ, 438, 876
Sion, E. M., Bänsicke, B. T., Long, K. S., Szkody, P., Knigge, C., Hubeny, I., deMartino, D., & Godon, P. 2008, ApJ, 681, 543
Wade, R. A., & Hubeny, I. 1998, ApJ, 509, 350
Warner, B. 1995, Cataclysmic Variable Stars (Cambridge: Cambridge Univ. Press)
Wood, M. A. 1990, Ph.D. thesis, Univ. Texas at Austin